AIAA'85

AIAA-85-0043

Calculations of Interaction of Acoustic Waves with a Two-Dimensional Free Shear Layer

S. Koshigoe, Naval Weapons Center, China Lake, CA; and V. Yang and F.E.C. Culick, California Institute of Technology, Pasadena, CA

AIAA 23rd Aerospace Sciences Meeting

January 14-17, 1985/Reno, Nevada

CALCULATIONS OF INTERACTION OF ACOUSTIC WAVES WITH A TWO-DIMENSIONAL FREE SHEAR LAYER

S. Koshigoe[+]
Naval Weapons Center
China Lake, California 93555

and

V. Yang[*] and F. E. C. Culick[**]
California Institute of Technology
Pasadena, California 91125

Abstract

The acoustic/vortical interaction in a two-dimensional free shear layer has been studied. The flowfield is represented by division into two parts: the vortical and the compressible flows. Each field is treated separately and linked with the other through the Bernoulli enthalpy. Acoustic waves are identified as unsteady compressible motions free of vorticity. Calculations have been carried out for the flowfields with and without externally imposed disturbances. Preliminary results reported here indicate that the motion of large coherent flow structures contributes significantly to sound generation. In particular, the formation of large structure and subsequent pairing appear globally as a quadrupole source.

Nomenclature

a	speed of sound
G	Green's function
h	enthalpy
H	Bernoulli enthalpy, defined by Eq. (8)
$\mathbf{i}$	unit directional vector in x-coordinate
$\mathbf{j}$	unit directional vector in y-coordinate
$\mathbf{k}$	unit directional vector in z-coordinate
N	number of vortices in the computational domain
r_o	radius of vortex blob
t	time
u	axial velocity component
U	free stream velocity
$\mathbf{u}$	hydrodynamic flow velocity
v	vertical velocity component
$\mathbf{v}$	total flow velocity
$\mathbf{v}_c$	compressible flow velocity
$\mathbf{x}$	position coordinate
γ_1	vorticity distribution function
Γ	strength of vortex element
ω	vorticity
φ	total potential
φ_m	time averaged quantity of φ
φ_a	acoustic potential

subscripts

1	value of the high-speed free stream
2	value of the low-speed free stream

+ Research Engineer

* Research Fellow in Jet Propulsion

** Professor of Applied Physics and Jet Propulsion, Associate Fellow AIAA

1. Introduction

Recent studies of pressure oscillations in air breathing and rocket propulsion systems have indicated that the acoustic/vortical interaction may contribute actively to the excitation of flow instabilities. An existing small amplitude acoustic wave causes fluctuations of the intrinsically unsteady vortical flow, which in turn emanates an acoustic wave. If the process occurs at the proper time and position, a feedback loop and mutual coupling can be established and substantial oscillations may be produced.

So far very little is known about the detailed characteristics of the interactions. Experience with related work on aeroacoustics clearly demonstrates the complexity and uncertainty of the problem. Therefore, in the first instance, we shall restrict our attention only to the interactions involving plane acoustic waves propagating parallel to the plane of a two-dimensional free shear layer, illustrated in Figure 1. This simple configuration represents a generic model from which many complicated flows may arise. The purpose is to promote the basic understanding of the acoustic/vortical interaction with detailed calculations of (i) the conversion of acoustic fluctuation from unsteady vortical motion and (ii) the excitation of vortical flow by imposed acoustic disturbance.

The generation of acoustic oscillations in a free shear layer is a consequence of the intensive mixing between two uniform streams. Owing to the hydrodynamic instability, the mixing process is inherently unsteady and leads to vorticity to be shed from the trailing edge of the splitter plate. From a fundamental point of view, acoustic waves occur in a compressible medium with unsteady pressure fluctuations. The shear layer serves as a continuous source distribution. Systematic investigation of flow induced sound seems to have begun with an approach based on acoustic analogy introduced by Lighthill[1,2] to study jet noise. By splitting the density field into incompressible and acoustic parts, Lighthill was able to derive a forced wave equation in which turbulence provides a quadrupole sound source. A considerable number of schemes have appeared subsequently. They all use the acoustic analogy in one form or another, constructing a model for the source term and calculating the far field radiation. Detailed investigation of the flowfield has not been performed except for some simple model problems. The difficulty lies in the modeling and calculation of turbulent shear flows and their interactions with acoustic oscillations. General surveys on this subject have recently been given by Ffowcs Williams,[3] Crighton,[4] and Goldstein.[5]

In the following, a general formulation of the flowfield is constructed, based on the concept of the Bernoulli enthalpy of Yates.[6] The flowfield is represented as a decomposition into the vortical and the compressible fields, using the Helmholtz splitting theorem. The vortical flow is considered incompressible and simulated with the Lagrangian vortex dynamics method. The distribution of vorticity is discretized and the velocity of each discrete vortex is calculated according to the Biot-Savart law. The influences of the compressible field appear in the convection of vortices. The acoustic oscillations are identified as unsteady compressible motions free of vorticity and tr[illegible] within linear analysis. They are governed by an [illegible]mogeneous wave equation accommodating the wave propagation, the interaction with the vortical disturbance, and the sound generation. For a homentropic flow, this equation can be conveniently solved by using a Green's function and finite difference methods.

Detailed calculations have been carried out for both the vortical and the acoustic fields. Results indicate that coherent vortex motion plays an essential role in sound generation. As a consequence of vortex clustering and pairing, a quadrupole sound source is produced. The analysis has also been conducted to study the effects of external acoustic disturbances on the flowfield. Owing to several approximations made to simplify the analysis, the results obtained here must be regarded as exploratory and preliminary. The chief purpose has been to initiate studies of the processes responsible for the generation of small amplitude acoustic waves by a free shear layer.

2. Analysis

The analysis is based on the inviscid equations of motion for a homentropic fluid. Since it is more convenient to distinguish sound radiation from its source through the enthalpy field than the other thermodynamic fields, the following conservation equations are considered.

$$\frac{1}{a^2}\frac{Dh}{Dt} + \nabla\cdot\mathbf{v} = 0 \qquad (1)$$

$$\frac{D\mathbf{v}}{Dt} + \nabla h = 0 \qquad (2)$$

where the operator D/Dt denotes the material derivative, $\partial/\partial t + \mathbf{v}\cdot\nabla$.

To formulate the hydrodynamic and the acoustic flows separately, we decompose the flow velocity $\mathbf{v}$ into solenoidal and irrotational parts.

$$\mathbf{v} = \mathbf{u} + \mathbf{v}_c \quad \text{where} \quad \nabla\cdot\mathbf{u} = 0; \quad \mathbf{v}_c = \nabla\varphi \qquad (3)$$

The irrotational part is the velocity associated with fluid compressibility. Since only unsteady volume dilatation can generate sound, the total potential φ is further written as a sum of acoustic and nonacoustic parts.

$$\varphi(\mathbf{x},t) = \varphi_a(\mathbf{x},t) + \varphi_m(\mathbf{x}) \qquad (4)$$

Substitution of (3) and (4) into (1) produces an equation characterizing the acoustic potential φ_a.

$$\nabla^2\varphi_a = -\frac{1}{a^2}\frac{Dh}{Dt} - \nabla^2\varphi_m = -\frac{1}{a^2}\frac{Dh}{Dt} + \left\langle \frac{1}{a^2}\frac{Dh}{Dt} \right\rangle \qquad (5)$$

where $\langle\ \rangle$ represents the time averaged quantity. As far as linear problems for φ is concerned, direct calculation of the acoustic potential φ_a is inefficient and unnecessary. For convenience, we choose the total potential φ as the primary variable and φ_a can be easily deduced by subtracting the time averaged value.

The equation for the total potential is constructed by suitably combining the conservation equations. Following the procedure described in reference 6 and collecting only linear terms for φ, we obtain

$$\frac{1}{a^2}\frac{\partial^2\varphi}{\partial t^2} - \nabla^2\varphi = \frac{1}{a^2}\frac{\tilde{D}H}{\tilde{D}t} - \frac{2}{a^2}\mathbf{u}\cdot\nabla\frac{\partial\varphi}{\partial t} - \frac{1}{a^2}\frac{\partial\mathbf{u}}{\partial t}\nabla\varphi \qquad (6)$$

where $\tilde{D}/\tilde{D}t$ is defined as $\partial/\partial t + \mathbf{u}\cdot\nabla$ and H is the Bernoulli enthalpy satisfying the following Poisson equation,

$$\nabla^2 H = \nabla\cdot[(\nabla\varphi + \mathbf{u})\times\omega - \nabla\,|\frac{\mathbf{u}}{2}|^2] \qquad (7)$$

$$H = h + \frac{\tilde{D}\varphi}{\tilde{D}t} + \frac{1}{2}(\nabla\varphi\cdot\nabla\varphi), \qquad (8)$$

These equations indicate that the Bernoulli enthalpy plays an essential role linking the acoustic and the hydrodynamic fields. The rate of change of H following the vortical motion provides the necessary energy for sound radiation. If the hydrodynamic flow is irrotational, no aerodynamic sources of sound may survive. Acoustic waves can be produced only by the unsteady motions of foreign bodies or boundaries. A detailed account of the significance of H has been given by Yates.[6]

To complete the analysis, the hydrodynamic field must be known. It is often easy to use vorticity as the primary variable. By taking the curl of (1) and substituting (3) into the result, the equation for the vorticity is obtained.

$$\frac{\partial \omega}{\partial t} + [(\mathbf{u} + \mathbf{v}_c)\cdot\nabla\,\omega] + (\nabla\cdot\mathbf{v}_c)\omega = 0 \tag{9}$$

Note that the vortex stretching term vanishes in this flow and ω is a vector normal to the xy-plane. For low frequency oscillations, the change of vorticity due to volume dilatation $(\nabla\cdot\mathbf{v}_c)\omega$ is negligibly small in comparison with that associated with compressible flow convection $\mathbf{v}_c\cdot\nabla\,\omega$. Therefore, to a good approximation the last term in (9) is ignored in subsequent calculations. The effect of compressibility appears only in the convection of vortices.

2.1 The Vortical Flow

The vortical field is approximated by the Lagrangian vortex dynamics method which treats vorticity as an assembly of vortex elements.

$$\omega(\mathbf{x},t) = \sum_{i=1}^{N}\Gamma_i\gamma_i(\mathbf{x} - \mathbf{x}_i(t)) \tag{10}$$

where Γ_i denotes the circulation (or strength) of the ith vortex element and γ_i is a two-dimensional function specifying the vorticity distribution inside each vortex element. Of various choices for the distribution function γ_i, the vortex blob method of Chorin[7] is used here for simplicity. This method bypasses the singularity associated with point vortex and in some sense perserves its mathematical significance. The complex velocity field induced by each blob is given by

$$u - iv = \frac{-i\Gamma_i}{2\pi}\frac{|z - z_i|}{\max(|z - z_i|, r_o)}\frac{1}{(z - z_i)} \tag{11}$$

where $z = x + iy$ and r_o is the radius of the blob within which the velocity magnitude is uniform. Substitute (10) into (9) and take the asymptotic limit of small r_o to find

$$\dot{\mathbf{x}}_i = \mathbf{u}(\mathbf{x}_i) + \mathbf{v}_c(\mathbf{x}_i) \tag{12}$$

This amounts to nothing more than the theorems of Helmholtz and Kelvin, the motion of vortex blob being determined by the local fluid velocity.

Numerical calculation of the vortical flow velocity $\mathbf{u}$ can usually be achieved either by the direct vortex interaction method according to the Biot-Savart law or by the cloud-in-cell method which solves the Poisson equation for the stream function. Each one has advantages complementary to the other; the choice depends on the features of the problem. In the present study, the direct method based on the Biot-Savart law is used as it provides a more faithful results and avoids the difficulties arising from the treatment of outer boundary conditions.

The numerical procedure is very similar to that taken by Spalart.[8] The region where vigorous mixing occurs defines the computational domain, ranging from the trailing edge of the splitter plate $\mathbf{x}=0$ to some downstream position at which the transport of vorticity in the negative $\mathbf{x}$-direction is negligible, as shown in Figure 1. At every time step, a vortex blob of strength $(U_1 - U_2)d$ is shed from the separation point, convected downstream with the local flow, and disappears when passing the right boundary. The flow outside the computational domain is simulated by two semi-infinite rows of vortices with fixed strength and positions. Consequently, from the Biot-Savart law the induced velocity at the ith blob $\mathbf{x}_i$ is given by

$$\mathbf{u}(\mathbf{x}_i) = \frac{-\Gamma}{2\pi}\sum_{j\neq i}^{\infty}\frac{(\mathbf{x}_i - \mathbf{x}_j)\times\mathbf{k}}{|\mathbf{x}_i - \mathbf{x}_j|^2} + \frac{U_1 + U_2}{2}\mathbf{i} \tag{13}$$

where the summation contains contributions from vortices both inside and outside the computational domain.

Within the present framework, the model suffers several deficiencies. First, the real flow is basically three-dimensional. The assumption of two-dimensionality may fail especially for high Reynolds number flows in which the spanwise disturbances can reach significant level. Second, although the mixing process is nearly inviscid, viscous effects play an important role in determination of the state of boundary layers on the splitter plate. Recent investigations[9] have shown that the downstream development of shear layers depends greatly on the state of the boundary layer. In addition, significant negative excursions in the instantaneous vorticity may occur due to the shedding of viscous boundary layers.[10] Third, perhaps the most importantly, the upstream boundary condition is not treated properly. The velocity component normal to the splitter plate does not vanish. Modification of this matter is currently being made by distributing a layer of doublets on the plate with strength determined as part of the solution to the entire problem.

2.2 The Acoustic Flow

The Bernoulli enthalpy needs to be specified first in order to solve the inhomgeneous wave equation (6). With the use of the vortex blob method, the solution to the Poisson equation (7) can be conveniently expressed in terms of Green's function chosen to satisfy the same differential operator.

$$\nabla^2 G = -\delta(\mathbf{x} - \mathbf{x}') \tag{14}$$

If we ignore the presence of the splitter plate, the Green's function in free space becomes

$$G(\mathbf{x}|\mathbf{x}') = \frac{-1}{2\pi}\ln|\mathbf{x} - \mathbf{x}'| \tag{15}$$

Multiply (7) by G, (14) by H, substract and integrate over the whole space to find

$$\int[G\nabla^2 H - H\nabla^2 G]ds = H(\mathbf{x}) + \int G\{\nabla\cdot[(\nabla\varphi + \mathbf{u})\times\omega - \nabla|\frac{\mathbf{u}}{2}|^2]\}ds \tag{16}$$

Since the vorticity is confined to a finite region and the acoustic wave vanishes at infinity, application of the Green's theorem yields

$$H(\mathbf{x}) = -\int G\{\nabla\cdot[(\nabla\varphi + \mathbf{u})\times\omega - \nabla|\frac{\mathbf{u}}{2}|^2]\}ds + h_\infty \tag{17}$$

where h_∞ is the free stream enthalpy. This equation can be further simplified by substituting (15) and using the divergence theorem twice to give

$$H(\mathbf{x}) = -\frac{\mathbf{u}\cdot\mathbf{u}}{2} + \frac{1}{2\pi}\int \frac{(\mathbf{x}-\mathbf{x}')\cdot[(\nabla\varphi + \mathbf{u})\times\omega]}{|\mathbf{x}-\mathbf{x}'|^2}ds + (h_\infty + \frac{U_1^2 + U_2^2}{4}) \tag{18}$$

Substitution of (10) in the above equation leads to

$$H(\mathbf{x}) = -\frac{\mathbf{u}\cdot\mathbf{u}}{2} - \frac{\Gamma}{2\pi}\sum_j^{\infty} \frac{(\mathbf{x}-\mathbf{x}_j)\times\mathbf{k}}{|\mathbf{x}-\mathbf{x}_j|^2}\cdot[\nabla\varphi_j + \mathbf{u}_j] + (h_\infty + \frac{U_1^2 + U_2^2}{4}) \tag{19}$$

The subscript j stands for the flow quantity at $\mathbf{x}_j$.

The source term $\tilde{D}H/\tilde{D}t$ can be determined now by taking the material derivative of (19). Following some straightforward manipulation, we get

$$\frac{\tilde{D}H}{\tilde{D}t} = \frac{\Gamma}{2\pi}\sum_j^N(\Delta\mathbf{u}_j - \nabla\varphi_j)\cdot\left[\frac{\Delta\mathbf{u}_j\times\mathbf{k}}{|\Delta\mathbf{x}_j|^2} - \frac{2(\Delta\mathbf{u}_j\cdot\Delta\mathbf{x}_j)\Delta\mathbf{x}_j\times\mathbf{k}}{|\Delta\mathbf{x}_j|^4}\right] - \frac{\Gamma}{2\pi}\sum_j^N\frac{\Delta\mathbf{x}_j\times\mathbf{k}}{|\Delta\mathbf{x}_j|^2}\cdot\left[\frac{\tilde{D}}{\tilde{D}t}\nabla\varphi_j - \frac{\Gamma}{2\pi}\sum_l^N\left(\frac{\Delta\mathbf{u}_{jl}\times\mathbf{k}}{|\Delta\mathbf{x}_{jl}|^2} - \frac{2(\Delta\mathbf{u}_{jl}\cdot\Delta\mathbf{x}_{jl})\Delta\mathbf{x}_{jl}\times\mathbf{k}}{|\Delta\mathbf{x}_{jl}|^4}\right)\right] \tag{20}$$

where $\Delta\mathbf{x}_j = \mathbf{x} - \mathbf{x}_j;\quad \Delta\mathbf{u}_j = \mathbf{u} - \mathbf{u}_j;$

$\Delta\mathbf{x}_{jl} = \mathbf{x}_j - \mathbf{x}_l;\quad \Delta\mathbf{u}_{jl} = \mathbf{u}_j - \mathbf{u}_l;$

Thus, we have completed the formulation for the compressible flowfield. The wave equation (6) is solved using a standard finite differene scheme with center differences for both time and spatial derivatives.

3. Discussion of Results

Calculations have been carried out to study the flowfields with and without externally imposed acoustic disturbances. Both cases have the same free stream velocities, 50 m/sec in the upper and 30 m/sec in the lower sides. The computational domain spans a region up to 0.64 m downstream of the splitter plate. Because the acoustic wave interacts with the hydrodynamic field, the time step Δt used in the calculation of vortex motions can not be determined arbitrarily. It has to comply with the stability criterion required for the numerical solution to the inhomgeneous wave equation (6). In the grid system used here, Δt is chosen to be 37 μsec. As a result, there are about 410 vortices in the computational domain.

Case 1. No External Excitation

This case serves as a baseline for the entire work and should be tested with available experimental data. Figure 2 shows the discrete vortex motion at various times in a reference frame moving with the mean flow. The coalescence of vortices into coherent flow structure is clearly seen. To make a direct comparison with experimental measurement, a spectral analysis of fluctuating velocities is conducted. Results for the Strouhal number based on the initial mometum thickness agrees well with the prediction by linear stability theory.[11] The shedding frequency is about 500 Hz.

Figure 3 shows the distributions of the acoustic source $\tilde{D}H/\tilde{D}t$ at two different times. The solid and the dashed lines denote the positive and the negative values respectively. A quadrupole structure begins to form at the position corresponding to the vortex roll-up, changing its shape and strength when moving downstream. Upstream of the vortex roll-up, no obvious acoustic source is observed. This implies that the large coherent eddies contribute actively to sound generation. The fixed dipole configuration at the plate edge is believed to be due to the failure to satisfy of the upstream boundary conditions, as discussed earlier.

Figure 4 shows the distributions of the acoustic potential φ_a at four different times, obtained by extracting the unsteady part of the total potential φ. The source region is complicated but in a broad sense governed by a quadrupole distribution. The dominant frequency 500 Hz matches the primary frequency of the vortical flow. Since the influences of the splitter plate on sound reflection and diffraction have been neglected, the far field acoustic wave has a clean circular shape.

Case 2. Imposed Acoustic Excitation

To study the effects of external excitation on the flowfield, we impose a plane acoustic disturbance at the edge of the plitter plate, as shown in Figure 1. The amplitude of the acoustic velocity is one percent of the mean flow value and the frequency is 1000 Hz. Figure 5 shows the vortex evolution in the mixing layer. The external forcing affects the downstream vortical motion considerably. The growth of the large eddy size is clearly suppressed.

Figure 6 shows the distributions of the acoustic potential at four different times. The flow pattern is very similar to the previous case. However, the strength becomes much weaker. The cause for this phenomenon is not clear; it may be due to the suppression of the vortex motion.

4. Concluding Remarks

A formal framework has been constructed to study the acoustic/vortical interaction in a two-dimensional free shear layer. The results obtained here must be regarded as only a beginning owing to several approximations incorporated in the analysis. In particular, because the boundary conditions on the splitter plate are not correctly satisfied, the analysis essentially simulates part of the flowfield, a deficiency which is the subject of continuing work. With these caveats, it appears that the formation of coherent structures, and subsequent pairing, cause the free shear layer to act as a quadrupole source of acoustic waves. Details of the processes remain to be clarified.

Acknowledgments

This work contains some results obtained from the research program supported partly by the Naval Weapons Center, partly by the California Institute of Technology, and partly by NAVAIR, Contract No. N0014-84-K-0434.

References

1. Lighthill, M. J., "On Sound Generated Aerodynamically: I.-General Theory," *Proceedings of Royal Society, London, Series A*, Vol.211, 1952, pp.564-587.
2. Lighthill, M. J., "On Sound Generated Aerodynamically: II.-Turbulence as a Source of Sound," *Proceedings of Royal Society, London, Series A*, Vol.222, 1954, pp.1-32.
3. Ffowcs Williams, J. E., "Aeroacoustics," *Annual Review of Fluid Mechanics*, 1977, pp. 447-468.
4. Crighton, D. G., "Acoustics as a Branch of Fluid Mechanics," *Journal of Fluid Mechanics*, Vol.106, 1981, pp.261-298.
5. Goldstein, M. E., "Aeroracoustics of Turbulent Shear Flows," *Annual Review of Fluid Mechanics*, 1984, pp. 263-285.
6. Yates, J. E.,"Application of the Bernoulli Enthalpy Concept to the Study of Vortex Noise and Jet Impingement Noise," *NASA-CR-2987*, 1978.
7. Chorin, A. J., "Numerical Studies of Slight Viscous Flow," *Journal of Fluid Mechanics*, Vol.57, 1973, pp.785-796.
8. Leonard, A., "Vortex Methods for Flow Simulation," *Journal of Computational Physics*, Vol.37, No.3, 1980, pp.289-335.
9. Ho, C.-M. and Huerre, P., "Perturbed Free Shear Layers," *Annual Review of Fluid Mechanics*, 1984, pp. 365-424.
10. Lang, D. B., "Laser Doppler Velocity and Vorticity Measurements in Turbulent Shear Layers," Ph.D. Thesis, California Institute of Technology, 1985.
11. Michalke, A., "On Spatially Growing Disturbance in an Inviscid Shear Layer," *Journal of Fluid Mechanics*, Vol.23, 1965, pp.521-544.

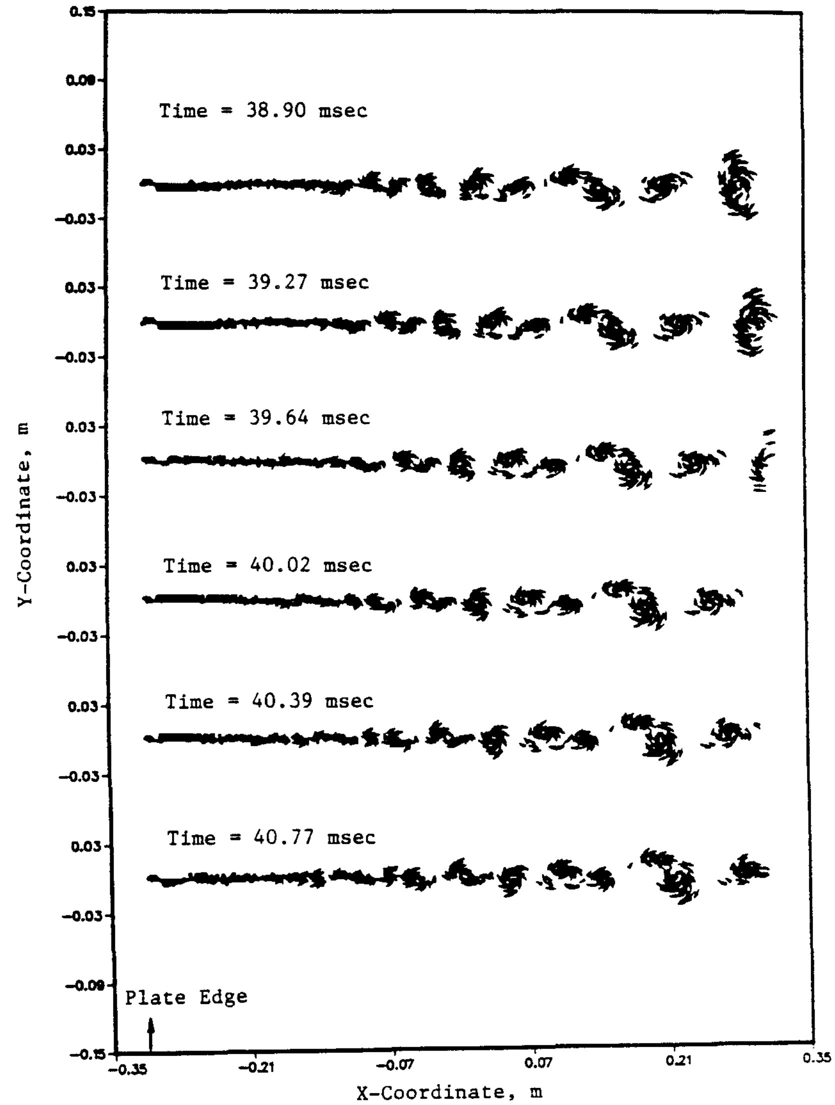

Figure 2. Discrete Vortex Motions at Various Times (Case 1. No External Excitation).

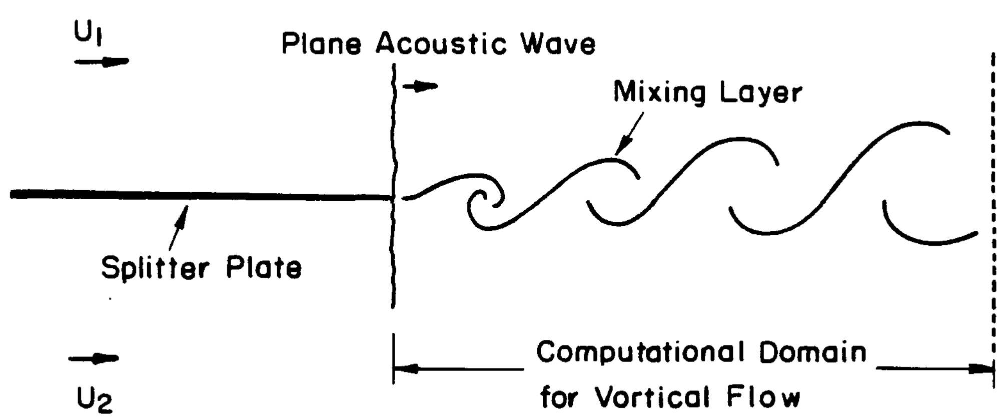

Figure 1. Sketch of a Two-Dimensional Free Shear Layer with a Plane Acoustic Wave

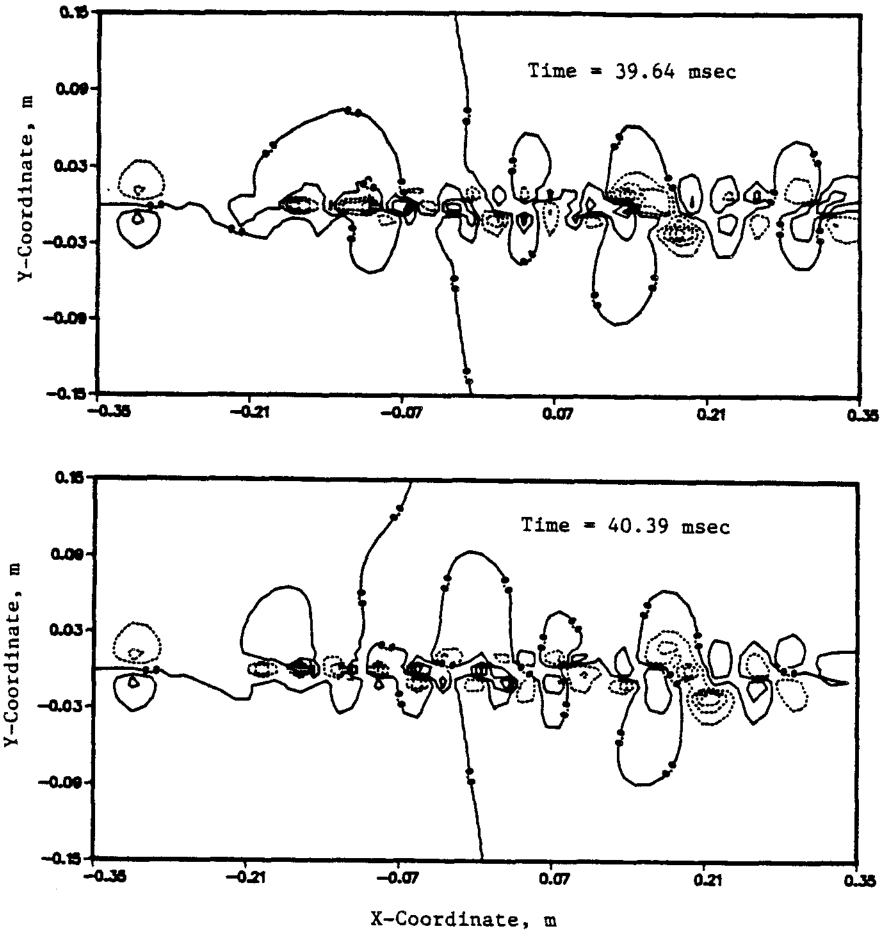

Figure 3. Distributions of the Acoustic Source $\tilde{D}H/\tilde{D}t$ at Various Times (Case 1. No External Excitation).

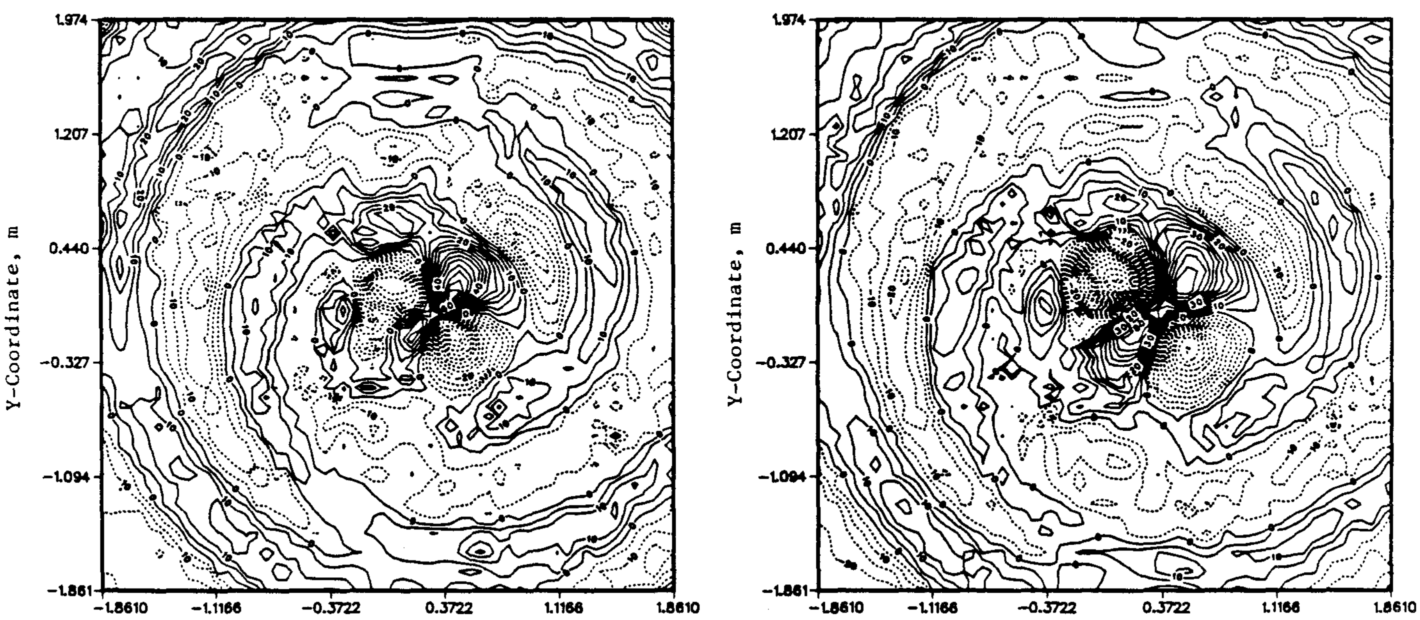

4a) 4b)

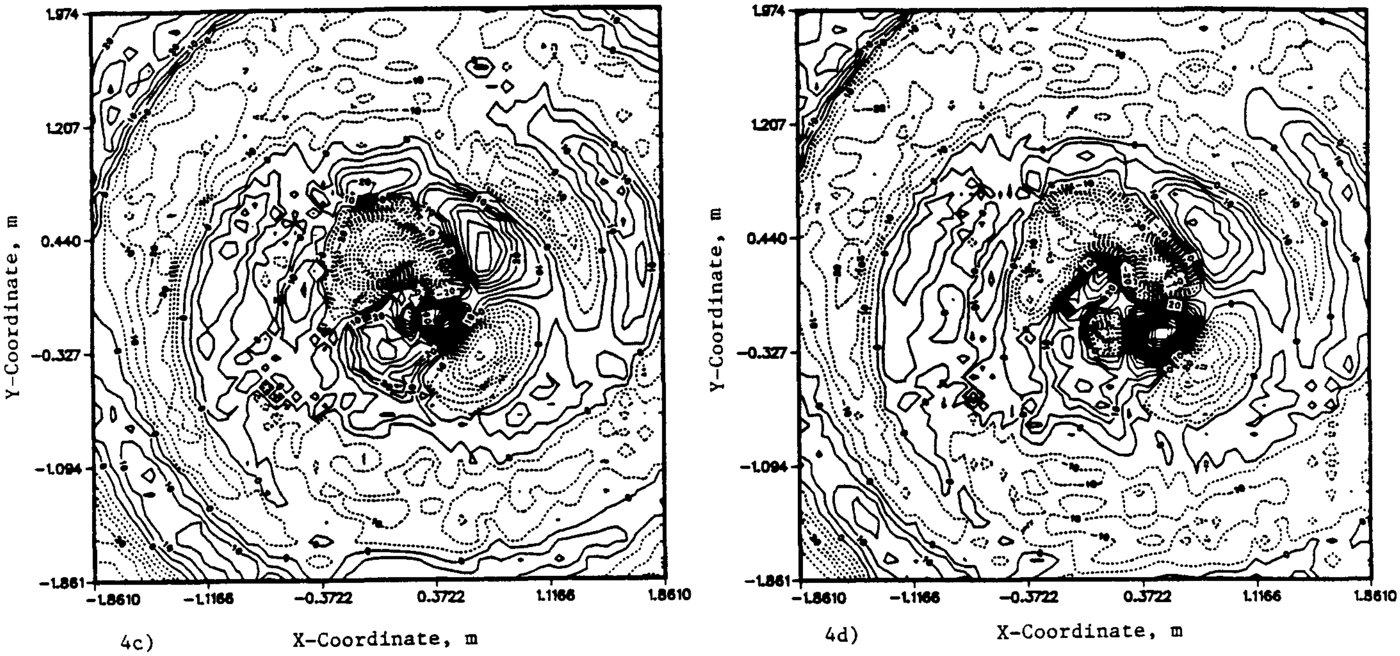

Figure 4. Distributions of the Acoustic Velocity Potential at Various Times (Case 1. No External Excitation). a) Time =39.27 ms; b) Time = 39.64 ms; c) Time = 40.02 ms; d) Time = 40.39 ms.

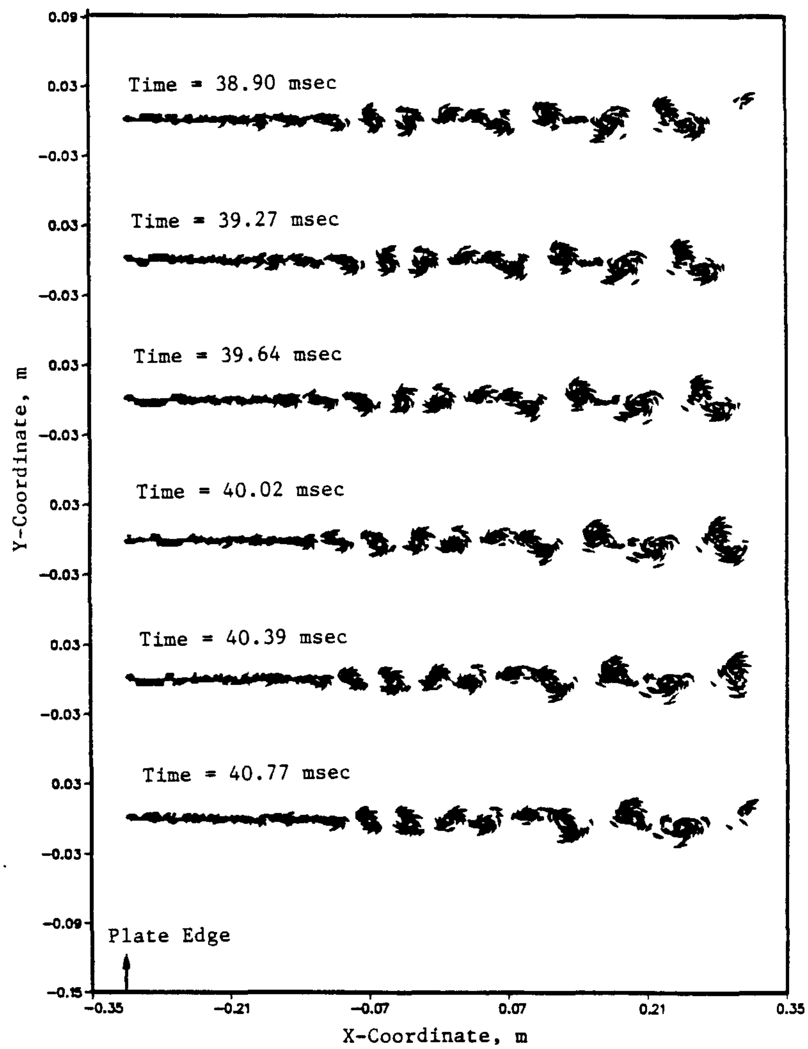

Figure 5. Discrete Vortex Motions at Various Times (Case 2. Imposed Acoustic Disturbance)

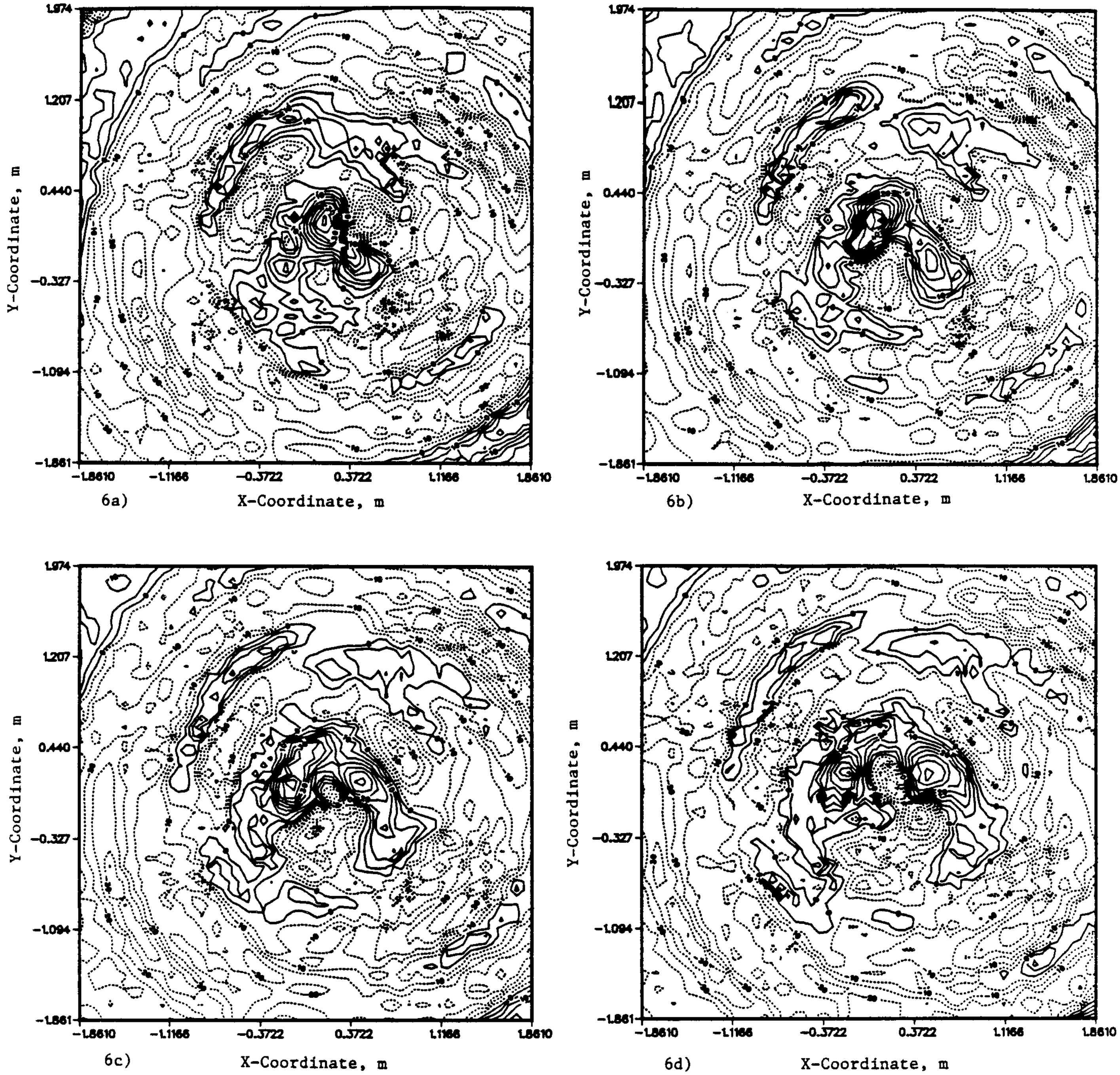

Figure 6. Distributions of the Acoustic Velocity Potential at Various Times (Case 2. Imposed Acoustic Disturbance). a) Time = 39.27 ms; b) Time = 39.64 ms; c) Time = 40.02 ms; d) Time = 40.39 ms.